HHS Public Access

Author manuscript

Nat Cell Biol. Author manuscript; available in PMC 2013 May 01.

Published in final edited form as:

Nat Cell Biol. 2012 November ; 14(11): 1212–1222. doi:10.1038/ncb2607.

Elf5 inhibits epithelial mesenchymal transition in mammary gland development and breast cancer metastasis by transcriptionally repressing Snail2/Slug

Rumela Chakrabarti[1,2], **Julie Hwang**[1,#], **Mario Andres Blanco**[1,#], **Yong Wei**[1], **Martin Lukačišin**[1], **Rose-Anne Romano**[2], **Kirsten Smalley**[2], **Song Liu**[3], **Qifeng Yang**[4,5,6], **Toni Ibrahim**[7], **Laura Mercatali**[7], **Dino Amadori**[7], **Bruce G. Haffty**[4,5], **Satrajit Sinha**[2,*], and **Yibin Kang**[1,5,*]

[1]Department of Molecular Biology, Princeton University, Princeton, NJ 08544

[2]Department of Biochemistry, Center of Excellence in Bioinformatics and Life Sciences, State University of New York at Buffalo, Buffalo, NY 14203

[3]Department of Biostatistics, Roswell Park Cancer Institute, Buffalo, NY 14263, USA

[4]Department of Radiation Oncology, Robert Wood Johnson Medical School, University of Medicine and Dentistry of New Jersey, New Brunswick, NJ 08901, USA

[5]Cancer Institute of New Jersey, New Brunswick, NJ 08903, USA

[7]Osteoncology Center, Istituto Scientifico Romagnolo per lo Studio e la Cura dei Tumori (I.R.S.T.), Meldola, Italy

Abstract

Epithelial–mesenchymal transition (EMT) is a complex process which occurs during organogenesis and in cancer metastasis. Despite recent progress, the molecular pathways connecting the physiological and pathological functions of EMT need to be better defined. Here we show that the transcription factor Elf5, a key regulator of mammary gland alveologenesis, controls EMT in both mammary gland development and metastasis. We uncovered this role of Elf5 through analyses of Elf5 conditional knockout animals, various *in vitro* and *in vivo* models of EMT and metastasis, an MMTV-neu transgenic model of mammary tumor progression, and clinical breast cancer samples. Furthermore, we demonstrate that Elf5 suppresses EMT by directly

[*]Corresponding Authors Communications to: Yibin Kang, Ph.D, Department of Molecular Biology, Princeton University, Washington Road, LTL 255, Princeton, NJ 08544, Phone: (609) 258-8834, Fax: (609) 258-2340, ykang@princeton.edu. Satrajit Sinha, Ph.D., Department of Biochemistry, State University of New York, 701 Ellicott Street, Buffalo, NY 14203, Phone: (716) 881-7994, FAX: (716) 849-6655, ssinha2@buffalo.edu.

[#]Equal contribution;

[6]Present address: Department of Breast Surgery, Qilu Hospital of Shandong University, Jinan, Shandong Province 250012, China

AUTHOR CONTRIBUTIONS

R.C., S.S. and Y.K. designed experiments. R.C., M.A.B., J.H., Y.W. and M.L. performed the experiments. R.R., K.S., S. L., Q. Y., T.I., L.M., D. A., B.G.H., provide technical support. R.C., M.A.B. and Y.K. wrote the manuscript. All authors discussed the results and commented on the manuscript.

COMPETING FINANCIAL INTERESTS

The authors declare no competing financial interests.

repressing the transcription of Snail2/Slug, a master regulator of mammary stem cells and a known inducer of EMT. These findings establish Elf5 not only as a key cell lineage regulator during normal mammary gland development, but also as a suppressor of EMT and metastasis in breast cancer.

Epithelial-mesenchymal transition (EMT) is a process that is associated with dramatic changes in cell adhesion, polarity, and migratory properties, and is typically characterized by an up-regulation of mesenchymal markers such as Vimentin and a down-regulation of epithelial markers such as E-cadherin[1–6]. EMT and its reverse process — mesenchymal-epithelial transition (MET) — have been shown to be of critical importance in developmental and tissue remodeling processes such as mesoderm and neural crest formation, heart valve development, secondary palate formation, and wound healing[1–6]. Accumulating evidence from experimental and clinical studies also suggests that EMT plays an important role in tumor invasion and metastasis by endowing cells with a more motile, invasive phenotype[1, 2, 4, 7–9]. Given the complexity and dynamic nature of EMT and MET, it is not surprising that several signaling pathways important for both normal and cancer development, including the TGFβ, Wnt, Notch, EGF and FGF pathways, have been implicated in governing these transitions[2, 4, 9]. More recently, several non-coding RNAs such as miR200 and miR205 have also been shown to be involved in EMT[10–13]. These pathways often exert their effect on EMT by regulating the expression of crucial EMT-related transcription factors, including those belonging to the Snail family, ZEB1, ZEB2, and Twist1/2[2, 4, 14–18]. However, despite recent progress, the molecular mechanisms acting upstream of these factors in different physiological and pathological contexts are not well characterized[3, 5, 18, 19]. Recent studies have also highlighted a link between EMT and the induction of stem cell-like properties, particularly in mammary epithelial models[20, 21]. For example, it was recently reported that the EMT-inducing transcription factor Snail2 (also known as Slug, hereafter referred to as Snail2) is a master regulator of mammary stem cells (MaSCs) and cancer stem cells (CSCs)[20]. Thus, uncovering the regulatory mechanisms of EMT-related transcription factors should provide greater insight into the signaling programs that govern the multiple facets of mammary gland biology and tumorigenesis.

The transcription factor E74-like factor 5 (Elf5, also known as ESE-2) belongs to the Ets (E twenty-six)-domain transcription factor family[22, 23]. Ets family proteins regulate a wide spectrum of biological processes and not only contribute to physiological development and differentiation, but also possess oncogenic or tumor suppressive activities[24–27]. Indeed, several Ets factors has been associated with cancer initiation, progression and metastasis[24–26, 28–30], and expression of the Ets family member PDEF is lost in many epithelial cancers[31]. Similarly, recent studies have shown that loss of Elf5 is frequently observed in human breast cancer tissues and cell lines[32, 33], suggesting a potential tumor suppressive role for this transcription factor.

The importance of Elf5 in normal mammary gland development is evidenced by lactation failure and a blocked alveolar morphogenesis phenotype observed in Elf5 knockout female mice[34–36]. In addition to the well established role of Elf5 in alveologenesis, we have also recently reported that loss of Elf5 triggers an increase in MaSCs during normal mammary

gland development[37]. While these studies have firmly established Elf5 as a master regulator of cell fate determination in the mammary gland, the functional role of Elf5 in breast cancer progression remains largely unknown. Here, we used Elf5 conditional knockout animals, multiple breast cancer models, and clinical patient samples to uncover a unique role of Elf5 in suppressing EMT and metastasis via direct transcriptional repression of Snail2 in both the mammary gland epithelium and in breast cancer.

RESULTS

Elf5 knockout induces EMT in mouse mammary epithelium

ELF5-KO mammary glands exhibit completely blocked alveologenesis during pregnancy and lactation that is accompanied by increases in luminal progenitors cells[35, 36]. Elf5 loss also triggers increases in MaSCs during normal mammary gland development[37]. Given the proposed relationship between EMT and MaSCs[21], we asked whether Elf5-KO affected the epithelial characteristics of mammary gland tissue. We observed that the mammary epithelium of Elf5-KO animals exhibited weaker and patchier E-cadherin staining in the adherens junctions compared to wild type (WT) animals at two pregnancy stages (P12.5 and P17.5) and on lactation day 1 (Fig. 1a–f, Supplementary Table S1). Expression of the mesenchymal marker Vimentin as well as the crucial EMT inducer Snail2 was increased in Elf5-KO compared to WT luminal cells as shown by immunostaining (Fig. 1g–r, Supplementary Fig. S1a–e) and western blot analyses (Supplementary Fig. S1f), suggesting that absence of Elf5 induces mammary epithelial cells to undergo EMT-like phenotypic changes.

To evaluate whether Elf5-KO induced global EMT-related changes, we performed gene expression profiling on mammary glands at lactation day 1. Microarray analyses indicated that loss of Elf5 led to several molecular features of EMT, including upregulation of key transcriptional inducers such as *Twist1*, *Twist2*, *Zeb1*, *Zeb2*, and *Snai2* (Fig. 2a, Supplementary Fig. S1g, and Table S2). Importantly, these changes were also observed in microarrays performed specifically on mammary epithelial cells (MECs) purified from WT and Elf5-KO animals (Supplementary Fig. S1h). Furthermore, gene set enrichment analysis (GSEA) indicated that four distinct EMT/CSC-related gene signatures[38–41] were significantly enriched in Elf5-KO mammary epithelial tissue, strongly suggesting that Elf5 loss induces a pervasive and sustained EMT signaling program (Fig. 2b).

Next, to directly test the functional role of Elf5 in EMT, we stably overexpressed HA epitope tagged Elf5 (HA-Elf5) in NMuMG mouse mammary epithelial cells (Fig 2c) and evaluated its effects on TGFβ-induced EMT. While control cells underwent dramatic EMT within 72 hours of TGFβ treatment, Elf5-overexpressing cells retained their epithelial features and formed tighter clusters (Fig. 2d). Accordingly, E-cadherin expression was retained in TGFβ-treated Elf5-overexpressing cells but lost in control cells, regardless of cell culture density (Fig. 2d, e and Supplementary Fig. S1i). HA-Elf5 expression did not affect apoptosis in basal or TGFβ-treated conditions (Supplementary Fig. S1j). We further found that enforced HA-Elf5 expression blocked the TGFβ-induced upregulation of numerous mesenchymal genes and transcription factors, such as *Cdh2*, *Snai2*, *Twist1*, *Twist2*, *Zeb1* and

Zeb2 (Fig 2f). Taken together, these data suggest a functional role for Elf5 in inhibiting EMT in the mammary epithelium.

Elf5 knockdown in epithelial-like T47D breast cancer cells induces EMT

To investigate whether Elf5 also regulates EMT in the context of breast cancer, we analyzed Elf5 expression patterns in a panel of breast cancer cell lines[42]. We found that *EFL5* expression was significantly reduced in cell lines characterized by both mesenchymal morphology and high metastatic potential, suggesting the potential inhibitory role of Elf5 in EMT and metastasis (Supplementary Fig. S2a). To test this possibility experimentally, we used siRNAs to knock down Elf5 in epithelial-like T47D cells, which have moderate basal levels of Elf5 expression (Supplementary Fig. S2a and Fig. 3a–c). Elf5 knock down induced EMT-like morphological features, such as a spindle-shaped appearance (Fig. 3d), and led to significant reductions in E-CADHERIN, β-CATENIN and ZO-1 expression as well as increase in VIMENTIN and N-CADHERIN expression (Fig. 3a–d). Moreover, E-CADHERIN and β-CATENIN were lost from cell-cell contacts and F-actin cables were reduced in Elf5-silenced cells (Fig. 3d). Functionally, silencing of Elf5 increased cell motility in response to Prolactin (Fig. 3e). As a complementary experiment, we induced an EMT-like process in T47D cells using the Jak kinase inhibitor AG-490[43] and investigated the effect on Elf5 expression. Here we observed that AG-490-induced EMT-like changes, including loss of cell adhesion and E-CADHERIN expression, were also accompanied by a dramatic decrease in Elf5 expression (Supplementary Fig. S2b–c). Collectively, these data suggest that ELF5 is an enforcer of the epithelial phenotype and an inhibitor of EMT in breast cancer.

Elf5 promotes mesenchymal-epithelial transition (MET) in MDA-MB-231 breast cancer cells

We next asked whether overexpression of Elf5 could reverse the highly metastatic, mesenchymal-like MDA-MB-231 (MDA-231) breast cancer cell line back to an epithelial state. MDA-231 cells do not express detectable endogenous Elf5 (Supplementary Fig. S3b and Fig. 4a), and enforced stable expression of HA-Elf5 (MDA-231-Elf5; Fig. 4a and Supplementary Fig. S3b) led to an increased cuboidal and clustered appearance within 72 hr post-transduction (Fig. 4b). In agreement with the change in cellular appearance, HA-Elf5 overexpression increased the expression of several epithelial markers, such as E-CADHERIN, β-CATENIN and ZO-1, and decreased the expression of the mesenchymal cell markers VIMENTIN and SNAIL2 (Fig. 4a). While Elf5-induced E-CADHERIN accumulated in the cytoplasm of MDA-231-Elf5 cells, upregulated β-CATENIN localized to cell-cell junctions as expected (Fig. 4c). Furthermore, MDA-231-Elf5 cels, but not control cells displayed clear F-actin cables as well as an increased appearance of tight junctions, as indicated by membrane localized ZO-1, suggesting overall that a functional MET had occurred (Fig. 4c). Elf5-induced MET was further confirmed in an additional mesenchymal-like cell line, HEK293 (Supplementary Fig. S3c, d), suggesting a general function of Elf5 in enforcing epithelial cellular characteristics.

We next analyzed the influence of Elf5 on the expression of well established EMT-related transcription factors at 48h (immediate response) and 12 days (delayed response) post-transduction of HA-Elf5 lentiviruses in MDA-231 cells (Fig. 4d, e). As expected, Elf5

overexpression was followed by increased expression of the epithelial maker *CDH1* and decreased expression of the mesenchymal markers *CDH2*, *FN1*, and *VIM* (Fig. 4d). Reduced expression of several EMT-related transcription factors, including *TWIST1*, *TWIST2 and SNAI2*, was observed at 12 days post-Elf5 overexpression (Fig. 4d); however, only *SNAI2* was significantly repressed at 48h post-transduction, implicating SNAIL2 as a potential direct target of Elf5 in MET initiation (Fig. 4e). Functionally, we observed that overexpression of Elf5 decreased the serum-responsive motility (Fig. 4f, 20 h) and invasiveness (Fig. 4g and 4h, 24 h and 48 h respectively) of MDA-231 cells. To exclude the possibility that these observed Elf5 cellular phenotypes resulted from genetic drift during lentiviral infection, we treated MDA-231-Elf5 cells with Elf5 siRNA (Supplementary Fig. S4a) and observed that the Elf5-induced cuboidal and clustered phenotype was completely eliminated within 72 hours post-treatment (Supplementary Fig. S4b), demonstrating that the reversal of the mesenchymal phenotype of MDA-231 cells was specifically due to HA-Elf5 expression.

Elf5 inhibits EMT via direct transcriptional repression of SNAI2

To test whether the observed Elf5 cellular phenotypes are dependent on Elf5 transcriptional activity, we stably overexpressed a DNA binding mutant (MT-Elf5) form of Elf5[44] in MDA-231 cells and found that only WT-Elf5 induced the cuboidal and clustered phenotype (Supplementary Fig. S4c–d). To further probe the molecular nature and specificity of the Elf5-induced changes, we next performed microarray analyses on WT and MT MDA-231-Elf5 cells. GSEA confirmed the negative enrichment of EMT-related gene signatures in WT HA-Elf5 overexpressing compared to MT HA-Elf5 overexpressing cells (Supplementary Fig. S4e), suggesting that the observed MET-related phenotypes are dependent on the DNA binding ability of Elf5.

We next sought to identify the direct transcriptional targets of EMT among the established inducers of EMT. The transcription factor *SNAI2* was one of the candidate genes whose expression was consistently repressed by changes in Elf5 levels both in the mammary gland epithelium and in breast cancer cells (Fig. 1m–r, 3a–b, 4a, and 4d). Furthermore, *SNAI2* is the only prominent EMT-related transcription factor that was strongly suppressed by Elf5 overexpression within 48 hours (Fig. 4e). We thus hypothesized that Elf5 may modulate epithelial phenotypes via direct suppression of *SNAI2* expression. To investigate this possibility, we performed chromatin immunoprecipitation (ChIP) of HA-Elf5 in MDA-231-Elf5 cells followed by qPCR of the *SNAI2* promoter and upstream regions (Fig. 5a, b and Supplementary Table S3). We found that HA-Elf5 ChIPs were enriched for a conserved *SNAI2* promoter region (P2), but not for upstream (P3–P7) or promoter proximal (P1) regions, suggesting that the P2 region contains the primary site for Elf5-binding *in vivo* (Fig. 5c). This region is well conserved across species and, importantly, contains a consensus Elf5 DNA-binding motif[45] (Fig. 5b).

To assess the potential for Elf5 regulation of other EMT transcription factors, we performed *in silico* bioinformatics analyses of their promoter regions and uncovered potential Elf5-responsive elements in the *TWIST1* and *SNAI1* regulatory regions. However ChIP-qPCR analyses revealed no significant enrichment of HA-Elf5 binding in these regions, suggesting

that *TWIST* and *SNAI1* are unlikely to be direct Elf5 targets in our experimental context (Supplementary Fig. S4f, g). To examine whether Elf5 can repress the *SNAI2* promoter, we transfected WT or mutant (mutation of the Elf5 motif in P2) *SNAI2* promoter reporter constructs into control or MDA-231-Elf5 cells. We found that Elf5 overexpression significantly repressed WT but not mutant *SNAI2* promoter activity (Fig. 5d). To rule out cell line-specific effects, we also overexpressed Elf5 in MCF7 cells and observed similar repression of the *SNAI2* reporter (Fig. 5e).

If *Snai2* is an important downstream mediator of the Elf5 mediated EMT/MET phenotype, we would expect restoration of SNAIL2 expression to revert Elf5-induced cellular changes back to the parental state. Indeed, overexpression of FLAG-SNAIL2 restored the original mesenchymal appearance of epithelial-like MDA-231-Elf5 cells (Fig. 5f, g). Accordingly, expression of epithelial markers such as E-CADHERIN, β-CATENIN and ZO-1 decreased and mesenchymal markers such as VIMENTIN and FN1 were increased in MDA-231-Elf5-SNAIL2 compared to MDA-231-Elf5 cells (Supplementary Fig. S5a–c). Additionally, restoration of ZO-1 membrane localization in MDA-231-Elf5 cells was lost in MDA-231-Elf5-SNAIL2 cells (Supplementary Fig. S5c), further suggesting a reversion of MET. Finally, overexpression of SNAIL2 also partially rescued the reduced motility of MDA-231-Elf5 cells (Fig. 5h). Collectively, these data suggest that Elf5-induced MET is mediated by direct repression of the key EMT inducer SNAIL2.

Negative correlation of ELF5 and SNAIL2 in clinical samples

To investigate whether our experimental findings could be relevant to the pathogenesis of human breast cancer, we examined Elf5 expression patterns in relevant microarray datasets that are publicly available. In two independent clinical datasets[46, 47], we found that *ELF5* expression was markedly reduced in hyperplasia and multiple breast tumor subtypes compared to corresponding matched healthy tissue (Fig. 6a, b). We next investigated whether ELF5 may also suppress SNAIL2 expression in the clinical setting. Querying the NKI295 dataset[48], we observed an inverse correlation between *ELF5* and *SNAI2* expression (Supplementary Fig. S6a). Interestingly, the degree of this anti-correlation increased markedly in ER- patients (Fig. 6c and Supplementary Fig. S6b). Additionally, immunostaining of ELF5 and SNAIL2 in a limited set of 25 primary breast tumors revealed a similar anti-correlation in expression ($r = -0.457$, $p = 0.0245$ based on staining intensity score; Pearson correlation) (Fig. 6d and Supplementary Fig. S6c). However, sample size limitations precluded clinical subtype-specific analyses of these expression patterns. We further evaluated the prognostic value of Elf5 and Snail2 in a large public clinical microarray database of breast tumors from 1354 patients[49] and found trends toward favorable prognoses for *ELF5* high patients and poor prognoses for *SNAI2* high patients (Figure 6e). Interestingly, the prognostic power of both genes was again dramatically increased in ER- patients, further suggesting clinical subtype-specific roles of the *ELF5*-*SNAI2* axis (Fig. 6e). The subtype-specific prognostic power of *ELF5* was also present in the NKI295 dataset, in which *ELF5* low ER- patients were found to have significantly reduced distant metastasis-free survival times compared to *ELF5* high ER-patients (Fig. 6f). When *ELF5* low and *SNAI2* high were used in combination, there was only a slight increase in the prognostic power ($p=0.010$, Supplementary Fig. S6d) compared to *ELF5* low alone

(p=0.013), possible due to the strong anti-correlation of *ELF5* and *SNAIL2* in ER- patients. Overall, our clinical data support the experimentally described role for ELF5 as a SNAIL2 repressor and further indicate that Elf5 may function to oppose breast cancer progression.

Elf5 inhibits breast cancer metastasis

To directly investigate whether Elf5 can suppress metastasis via its ability to inhibit EMT, we used the highly lung-metastatic LM2 subline of MDA-231[50]. We first confirmed that Elf5 overexpression (Supplementary Fig. S6e) had the same effects on LM2 cells as it did on MDA-231 cells. Indeed, Elf5 induced cuboidal, clustered cellular morphologies (Supplementary Fig. 6f), global negative enrichment of EMT gene signatures, and decreased motility in LM2 cells (Fig. 7a,b).

We next investigated the effect of Elf5 overexpression on lung metastasis. Luciferase-labeled control or Elf5-overexpressing LM2 cells were injected intravenously into nude mice and subjected to bioluminescent imaging (BLI). LM2-Elf5 cells exhibited reduced lung metastasis abilities even at early time points (Fig. 7c, d), implying that Elf5 may be negatively affecting the extravasation and/or early seeding of lung metastasis. Continued BLI monitoring revealed a further reduction of metastatic outgrowth in the lungs of animals injected with Elf5-overexpressing cells (Fig. 7c, d), and histological analyses indicated a ten-fold decrease in the number of metastatic lesions produced by LM2-Elf5 cells compared to the control cells (Fig. 7e, f). Taken together, these analyses show that Elf5 strongly inhibits breast cancer lung metastasis.

Considering the importance of the immune system in lung metastasis[51, 52], we extended our analysis to an immunocompetent mouse model of lung metastasis. We overexpressed Elf5 in 4T1 murine breast cancer cell line[53] (Supplementary Fig. 7a) and tested its ability to inhibit metastasis *in vivo*. Here we found that 4T1-Elf5 cells show decreased spontaneous (Fig. 7g–h, by mammary fat pad injection) as well as experimental (Supplementary Fig. S7b, by tail vein injection) lung metastasis without affecting primary tumor growth (Supplementary Fig. S7c). qRT-PCR analysis indicated downregulation of EMT genes such as *Cdh2*, *Snai2*, *Twist2* and *Zeb1* in 4T1-Elf5 compared to control cells (Supplementary Fig. S7d), again suggesting that Elf5 functions to oppose EMT-related gene expression programs. As Elf5 overexpression was also shown to downregulate *Snai2* in 4T1 cells (Supplementary Fig. S7a, d), we asked whether the restoration of SNAIL2 expression could rescue the inhibition of metastasis by Elf5. Accordingly, 4T1 cells overexpressing control vector, HA-Elf5, FLAG-SNAIL2 or both HA-Elf5 and FLAG-SNAIL2 (Supplementary Fig. S7e–g) were generated and used for lung metastasis assays. While Ef5 overexpression alone led to a significant reduction of lung metastasis (Fig. 7i, j), combinatorial overexpression of both Elf5 and SNAIL2 fully reverted this inhibition (Fig. 7i, j). Therefore, our studies suggest that the inhibition of metastasis by Elf5 is primarily mediated through Snail2 in 4T1 cells.

To complement our xenograft and allograft metastasis models, we next examined the effects of Elf5 on lung metastasis using the well established MMTV-neu transgenic mouse model[54]. In accordance with our earlier report[37], immunofluorescence analysis indicated that the Elf5 conditional knockout (Elf5-KO) MMTV-Neu primary tumors were Keratin-14^{+} whereas the WT tumors were Keratin-14^{-}/Keratin-8^{+} (Fig. 8a), suggesting a significant luminal to basal

cell fate change in tumor cells upon loss of Elf5. Interestingly, we also observed an increase in Snail2 expression in Elf5-KO/MMTV-Neu compared to WT/MMTV-Neu tumors (Fig. 8a). Similar to results obtained from xenograft and allograft models, here we observed that Elf5-KO/Neu transgenic mice displayed a clear trend of increased lung metastasis incidence (Fig. 8b), as well as significantly increased numbers of lung metastasis nodules (Fig. 8c) and greater lung lesion surface area (Fig. 8d, e) as compared to their WT/Neu counterparts. Furthermore, Snail2 expression was strongly increased in Elf5-KO/Neu (Fig. 8e) compared to WT/Neu lung metastasis lesions. Finally, these results were further confirmed by independent experiments in which Elf5 overexpressing primary tumor cells derived from MMTV-PyMT transgenic mice showed significantly decreased lung metastasis abilities without detectable changes in primary tumor growth following mammary fat pad injections in FVB mice (Supplementary Fig. S8). Overall, data from transgenic mice complement our findings from the NMuMG, MDA-231, and 4T1 cell line models and clinical breast cancer samples, strongly supporting the role of Elf5 as a metastasis-suppressing gene through direct targeting of Snail2.

DISCUSSION

Increasing evidence suggests that the normal genetic programs underlying various developmental processes can often be usurped in pathological conditions such as cancer metastasis[55, 56]. The functional role of epithelial-mesenchymal transition, a process crucial for embryonic organogenesis, serves as a leading example of this burgeoning paradigm[2, 4, 7]. Not surprisingly, physiological and pathological EMT share many common features and molecular regulators, and EMT studies in the context of both development and cancer may thus provide an integrative understanding of the pathological basis of malignancy.

Elf5 is well known as the master regulator of alveolar cell fate in mammary gland development[35, 36], and recent work from our laboratory suggests a more expansive role for Elf5 in inhibiting MaSC activity[37]. However, it was not previously known whether this role of Elf5 in influencing mammary cell fate could also impact the development and progression of mammary tumors. In this report, we delineate for the first time the role of Elf5 in regulating EMT and metastasis. We have used a combination of *in vitro* cellular systems, bioinformatic analyses, and multiple *in vivo* metastasis models to show that gain of Elf5 promotes a global acquisition of numerous epithelial characteristics and suppresses metastatic progression. Conversely, loss of Elf5 induces dramatic EMT and accelerates lung metastasis. Mechanistically we have shown that Elf5 regulates these cellular programs via its direct transcriptional repression of the key EMT transcription factor *SNAIL2*. Finally, clinical dataset analyses suggest that this Elf5-SNAIL2 signaling axis is intact in breast cancer patients and significantly affects patient prognosis, particularly in the ER- cohort. Additional clinical and functional analysis will be needed to investigate the molecular basis of this subtype-specific association and the potential involvement of ELF5-SNAIL2 axis in other subgroups of breast cancers.

Snail2 is a transcription factor conserved across species that has been shown to play an important role in EMT during gastrulation[5]. In the breast epithelium, Snail2 is normally expressed in the basal/stem cell-enriched population in both mice and humans[57] and has

been established as one of the most powerful mediators of EMT in mouse and human invasive carcinoma cells[19, 58–60]. Intriguingly, a recent study has demonstrated a critical role for Snail2 in regulating mammary stem cell (MaSC) and CSC activity, particularly in cooperation with the transcription factor Sox9[20]. While Snail2 expression is known to be lost during the transition from MaSCs to differentiated luminal cells[20], the underlying mechanism of this repression in normal mammary differentiation is unknown. Our current study indicates Elf5 as a crucial negative regulator of Snail2 in both mammary gland development and breast cancer. Adding to our recent observation that loss of Elf5 results in an increase in MaSC activity[37], we have further dissected the role of the Elf5-Snail2 axis in MaSC regulation by gain-of-function overexpression of Elf5. Elf5 overexpression decreased MaSC activity, which was reverted by overexpression of Snail2 (Supplementary Table S4). Conversely, the increased MaSC phenotype observed in Elf5-KO mammary epithelial cells was reversed by Snail2 knockdown (Supplementary Table S5). Taken together with our extensive analysis of the Elf5-Snail2 axis in EMT and metastasis, our results suggest that high expression of Elf5 in the differentiated luminal lineage inhibits Snail2 expression and basal cell properties, while loss of Elf5 not only induces EMT and increases Snail2 - dependent MaSC activity, but also promote breast cancer metastasis (Fig. 8f). Overall, these findings support previous work by Weinberg and others demonstrating a tight relationship between EMT and stemness[20, 21, 40, 41, 61]. Interestingly, GSEA of our microarray data indicated that there is significant enrichment of the CSC gene signature in Elf5-KO mouse mammary glands (Fig. 2b) and, correspondingly, negative enrichment of the CSC signature in Elf5-overexpressing breast cancer cells (Fig. 7a). Future experiments will be needed to investigate the potential role of Elf5 as an inhibitor of CSCs.

Altogether, our analyses have concluded that Elf5, through its direct negative regulation of Snail2, serves as a master enforcer of the epithelial cell fate. In the physiological context, this role promotes the proper identity of alveolar mammary epithelial cells, whereas in the pathological context Elf5 functions as a suppressor of EMT and cancer metastasis. Notably, Elf5 loss has been frequently detected during the early onset of disease progression at the stage of breast hyperplasia. This event may therefore represent one of the driving forces for early stage breast tumor cells to proceed with EMT and subsequent metastatic progression, thus highlighting the recently described Elf5-Snail2 axis as a potential target for early therapeutic intervention in breast cancer progression.

Supplementary Material

Refer to Web version on PubMed Central for supplementary material.

Acknowledgments

We thank M. Korpal, B. I. Koh, H. Zheng and B. Ell for helpful discussions, M. Yuan and X. Hang for technical assistance, C. DeCoste for assistance with flow cytometry, J. Goodhouse for assistance with confocal microscopy and L. Cong, J. Friedman at Tissue Analytic Service Core of Cancer Institute of New Jersey for assistance with clinical breast tumor sample IHC analysis. This research was supported by grants from R01GM069417 to S.S. and from the Brewster Foundation, the Champalimaud Foundation, and the National Institutes of Health (R01CA134519 and R01CA141062) to Y.K. R.C. is a recipient of a DOD postdoctoral fellowship (W81XWH-11-1-0681) and M.A.B. is a recipient of an NRSA pre-doctoral fellowship from the National Institutes of Health.

References

1. Thiery JP, Sleeman JP. Complex networks orchestrate epithelial-mesenchymal transitions. Nat Rev Mol Cell Biol. 2006; 7:131–142. [PubMed: 16493418]
2. Yang J, Weinberg RA. Epithelial-mesenchymal transition: at the crossroads of development and tumor metastasis. Dev Cell. 2008; 14:818–829. [PubMed: 18539112]
3. Lee JM, Dedhar S, Kalluri R, Thompson EW. The epithelial-mesenchymal transition: new insights in signaling, development, and disease. The Journal of cell biology. 2006; 172:973–981. [PubMed: 16567498]
4. Thiery JP, Acloque H, Huang RY, Nieto MA. Epithelial-mesenchymal transitions in development and disease. Cell. 2009; 139:871–890. [PubMed: 19945376]
5. Acloque H, et al. Reciprocal repression between Sox3 and snail transcription factors defines embryonic territories at gastrulation. Dev Cell. 2011; 21:546–558. [PubMed: 21920318]
6. Nieto MA. The ins and outs of the epithelial to mesenchymal transition in health and disease. Annual review of cell and developmental biology. 2011; 27:347–376.
7. Thompson EW, Williams ED. EMT and MET in carcinoma--clinical observations, regulatory pathways and new models. Clinical & experimental metastasis. 2008; 25:591–592. [PubMed: 18566898]
8. Thiery JP. Epithelial-mesenchymal transitions in tumour progression. Nature reviews Cancer. 2002; 2:442–454. [PubMed: 12189386]
9. Polyak K, Weinberg RA. Transitions between epithelial and mesenchymal states: acquisition of malignant and stem cell traits. Nature reviews Cancer. 2009; 9:265–273. [PubMed: 19262571]
10. Gregory PA, et al. The miR-200 family and miR-205 regulate epithelial to mesenchymal transition by targeting ZEB1 and SIP1. Nature cell biology. 2008; 10:593–601. [PubMed: 18376396]
11. Park SM, Gaur AB, Lengyel E, Peter ME. The miR-200 family determines the epithelial phenotype of cancer cells by targeting the E-cadherin repressors ZEB1 and ZEB2. Genes & development. 2008; 22:894–907. [PubMed: 18381893]
12. Korpal M, Lee ES, Hu G, Kang Y. The miR-200 family inhibits epithelial-mesenchymal transition and cancer cell migration by direct targeting of E-cadherin transcriptional repressors ZEB1 and ZEB2. The Journal of biological chemistry. 2008; 283:14910–14914. [PubMed: 18411277]
13. Burk U, et al. A reciprocal repression between ZEB1 and members of the miR-200 family promotes EMT and invasion in cancer cells. EMBO reports. 2008; 9:582–589. [PubMed: 18483486]
14. Medici D, Hay ED, Olsen BR. Snail and Slug promote epithelial-mesenchymal transition through beta-catenin-T-cell factor-4-dependent expression of transforming growth factor-beta3. Mol Biol Cell. 2008; 19:4875–4887. [PubMed: 18799618]
15. Wellner U, et al. The EMT-activator ZEB1 promotes tumorigenicity by repressing stemness-inhibiting microRNAs. Nature cell biology. 2009; 11:1487–1495. [PubMed: 19935649]
16. Yang J, et al. Twist, a master regulator of morphogenesis, plays an essential role in tumor metastasis. Cell. 2004; 117:927–939. [PubMed: 15210113]
17. Cano A, et al. The transcription factor snail controls epithelial-mesenchymal transitions by repressing E-cadherin expression. Nature cell biology. 2000; 2:76–83. [PubMed: 10655586]
18. Liu YN, et al. MiR-1 and miR-200 inhibit EMT via Slug-dependent and tumorigenesis via Slug-independent mechanisms. Oncogene. 2012
19. Liu YN, et al. Critical and reciprocal regulation of KLF4 and SLUG in transforming growth factor beta-initiated prostate cancer epithelial-mesenchymal transition. Molecular and cellular biology. 2012; 32:941–953. [PubMed: 22203039]
20. Guo W, et al. Slug and Sox9 cooperatively determine the mammary stem cell state. Cell. 2012; 148:1015–1028. [PubMed: 22385965]
21. Mani SA, et al. The epithelial-mesenchymal transition generates cells with properties of stem cells. Cell. 2008; 133:704–715. [PubMed: 18485877]
22. Sharrocks AD. The ETS-domain transcription factor family. Nat Rev Mol Cell Biol. 2001; 2:827–837. [PubMed: 11715049]

23. Hollenhorst PC, McIntosh LP, Graves BJ. Genomic and biochemical insights into the specificity of ETS transcription factors. Annual review of biochemistry. 2011; 80:437–471.
24. Desmaze C, et al. Multiple chromosomal mechanisms generate an EWS/FLI1 or an EWS/ERG fusion gene in Ewing tumors. Cancer Genet Cytogenet. 1997; 97:12–19. [PubMed: 9242212]
25. Dittmer J, Nordheim A. Ets transcription factors and human disease. Biochim Biophys Acta. 1998; 1377:F1–11. [PubMed: 9606973]
26. Peter M, et al. A new member of the ETS family fused to EWS in Ewing tumors. Oncogene. 1997; 14:1159–1164. [PubMed: 9121764]
27. Sharrocks AD, Brown AL, Ling Y, Yates PR. The ETS-domain transcription factor family. Int J Biochem Cell Biol. 1997; 29:1371–1387. [PubMed: 9570133]
28. Oikawa T, Yamada T. Molecular biology of the Ets family of transcription factors. Gene. 2003; 303:11–34. [PubMed: 12559563]
29. Sapi E, Flick MB, Rodov S, Kacinski BM. Ets-2 transdominant mutant abolishes anchorage-independent growth and macrophage colony-stimulating factor-stimulated invasion by BT20 breast carcinoma cells. Cancer Res. 1998; 58:1027–1033. [PubMed: 9500466]
30. Sementchenko VI, Schweinfest CW, Papas TS, Watson DK. ETS2 function is required to maintain the transformed state of human prostate cancer cells. Oncogene. 1998; 17:2883–2888. [PubMed: 9879994]
31. Feldman RJ, Sementchenko VI, Gayed M, Fraig MM, Watson DK. Pdef expression in human breast cancer is correlated with invasive potential and altered gene expression. Cancer Res. 2003; 63:4626–4631. [PubMed: 12907642]
32. Zhou J, et al. A novel transcription factor, ELF5, belongs to the ELF subfamily of ETS genes and maps to human chromosome 11p13-15, a region subject to LOH and rearrangement in human carcinoma cell lines. Oncogene. 1998; 17:2719–2732. [PubMed: 9840936]
33. Ma XJ, et al. Gene expression profiles of human breast cancer progression. Proceedings of the National Academy of Sciences of the United States of America. 2003; 100:5974–5979. [PubMed: 12714683]
34. Zhou J, et al. Elf5 is essential for early embryogenesis and mammary gland development during pregnancy and lactation. The EMBO journal. 2005; 24:635–644. [PubMed: 15650748]
35. Oakes SR, et al. The Ets transcription factor Elf5 specifies mammary alveolar cell fate. Genes & development. 2008; 22:581–586. [PubMed: 18316476]
36. Choi YS, Chakrabarti R, Escamilla-Hernandez R, Sinha S. Elf5 conditional knockout mice reveal its role as a master regulator in mammary alveolar development: failure of Stat5 activation and functional differentiation in the absence of Elf5. Developmental biology. 2009; 329:227–241. [PubMed: 19269284]
37. Chakrabarti R, et al. Elf5 regulates mammary gland stem/progenitor cell fate by influencing notch signaling. Stem Cells. 2012; 30:1496–1508. [PubMed: 22523003]
38. Herschkowitz JI, et al. Identification of conserved gene expression features between murine mammary carcinoma models and human breast tumors. Genome Biol. 2007; 8:R76. [PubMed: 17493263]
39. Gupta PB, et al. Identification of selective inhibitors of cancer stem cells by high-throughput screening. Cell. 2009; 138:645–659. [PubMed: 19682730]
40. Taube JH, et al. Core epithelial-to-mesenchymal transition interactome gene-expression signature is associated with claudin-low and metaplastic breast cancer subtypes. Proceedings of the National Academy of Sciences of the United States of America. 2010; 107:15449–15454. [PubMed: 20713713]
41. Blick T, et al. Epithelial mesenchymal transition traits in human breast cancer cell lines parallel the CD44(hi/)CD24 (lo/−) stem cell phenotype in human breast cancer. Journal of mammary gland biology and neoplasia. 2010; 15:235–252. [PubMed: 20521089]
42. Hoeflich KP, et al. In vivo antitumor activity of MEK and phosphatidylinositol 3-kinase inhibitors in basal-like breast cancer models. Clin Cancer Res. 2009; 15:4649–4664. [PubMed: 19567590]
43. Nouhi Z, et al. Defining the role of prolactin as an invasion suppressor hormone in breast cancer cells. Cancer Res. 2006; 66:1824–1832. [PubMed: 16452244]

44. Escamilla-Hernandez R, et al. Genome-wide search identifies Ccnd2 as a direct transcriptional target of Elf5 in mouse mammary gland. BMC Mol Biol. 2010; 11:68. [PubMed: 20831799]
45. Casas E, et al. Snail2 is an essential mediator of Twist1-induced epithelial mesenchymal transition and metastasis. Cancer Res. 2011; 71:245–254. [PubMed: 21199805]
46. Turashvili G, et al. Novel markers for differentiation of lobular and ductal invasive breast carcinomas by laser microdissection and microarray analysis. BMC Cancer. 2007; 7:55. [PubMed: 17389037]
47. Lee S, et al. Alterations of gene expression in the development of early hyperplastic precursors of breast cancer. Am J Pathol. 2007; 171:252–262. [PubMed: 17591970]
48. van de Vijver MJ, et al. A gene-expression signature as a predictor of survival in breast cancer. The New England journal of medicine. 2002; 347:1999–2009. [PubMed: 12490681]
49. Gyorffy B, et al. An online survival analysis tool to rapidly assess the effect of 22,277 genes on breast cancer prognosis using microarray data of 1,809 patients. Breast cancer research and treatment. 2010; 123:725–731. [PubMed: 20020197]
50. Minn AJ, et al. Genes that mediate breast cancer metastasis to lung. Nature. 2005; 436:518–524. [PubMed: 16049480]
51. DeNardo DG, et al. CD4(+) T cells regulate pulmonary metastasis of mammary carcinomas by enhancing protumor properties of macrophages. Cancer cell. 2009; 16:91–102. [PubMed: 19647220]
52. Kaplan RN, et al. VEGFR1-positive haematopoietic bone marrow progenitors initiate the pre-metastatic niche. Nature. 2005; 438:820–827. [PubMed: 16341007]
53. Miller FR, Miller BE, Heppner GH. Characterization of metastatic heterogeneity among subpopulations of a single mouse mammary tumor: heterogeneity in phenotypic stability. Invasion & metastasis. 1983; 3:22–31. [PubMed: 6677618]
54. Guy CT, et al. Expression of the neu protooncogene in the mammary epithelium of transgenic mice induces metastatic disease. Proceedings of the National Academy of Sciences of the United States of America. 1992; 89:10578–10582. [PubMed: 1359541]
55. Valastyan S, Weinberg RA. Tumor metastasis: molecular insights and evolving paradigms. Cell. 2011; 147:275–292. [PubMed: 22000009]
56. Sethi N, Kang Y. Dysregulation of developmental pathways in bone metastasis. Bone. 2011; 48:16–22. [PubMed: 20630490]
57. Lim E, et al. Transcriptome analyses of mouse and human mammary cell subpopulations reveal multiple conserved genes and pathways. Breast cancer research: BCR. 2010; 12:R21. [PubMed: 20346151]
58. Nieto MA. The snail superfamily of zinc-finger transcription factors. Nat Rev Mol Cell Biol. 2002; 3:155–166. [PubMed: 11994736]
59. Martin TA, Goyal A, Watkins G, Jiang WG. Expression of the transcription factors snail, slug, and twist and their clinical significance in human breast cancer. Ann Surg Oncol. 2005; 12:488–496. [PubMed: 15864483]
60. Proia TA, et al. Genetic predisposition directs breast cancer phenotype by dictating progenitor cell fate. Cell stem cell. 2011; 8:149–163. [PubMed: 21295272]
61. Battula VL, et al. Epithelial-mesenchymal transition-derived cells exhibit multilineage differentiation potential similar to mesenchymal stem cells. Stem Cells. 2010; 28:1435–1445. [PubMed: 20572012]

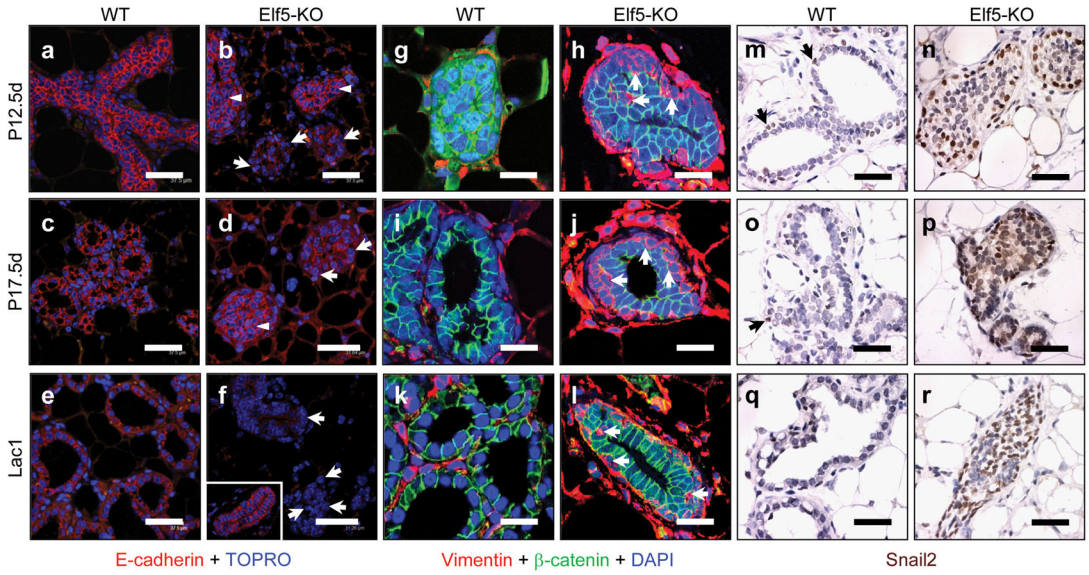

Figure 1. Loss of Elf5 in the mouse mammary gland results in an EMT-like phenotype during pregnancy and lactation

Analysis of the mouse mammary epithelium from wild type and Elf5-KO mice (n=5) revealed loss of E-cadherin ***(a–f)***, up-regulation of Vimentin ***(g–l)*** and nuclear Snail2 ***(m–r)*** in luminal epithelial cells during different stages of pregnancy. P12.5 in ***a, b, g, h, m, n***; P17.5 in ***c, d, i, j, o, p***; Lac1 in ***e, f, k, l, q, r***. Arrows indicate areas with loss of E-cadherin and arrowheads indicate areas with normal E-cadherin expression in ***a–f***. Inset in ***f*** shows adjacent mammary epithelium with normal expression of E-cadherin. White arrows in ***g–l*** show abnormal Vimentin expression in luminal epithelial cells. Black arrows in ***m–r*** show normal Snail2 protein localization in basal epithelial cells. Size bar = 40 μm in ***a–f, m–r*** and 18 μm in ***g–l***.

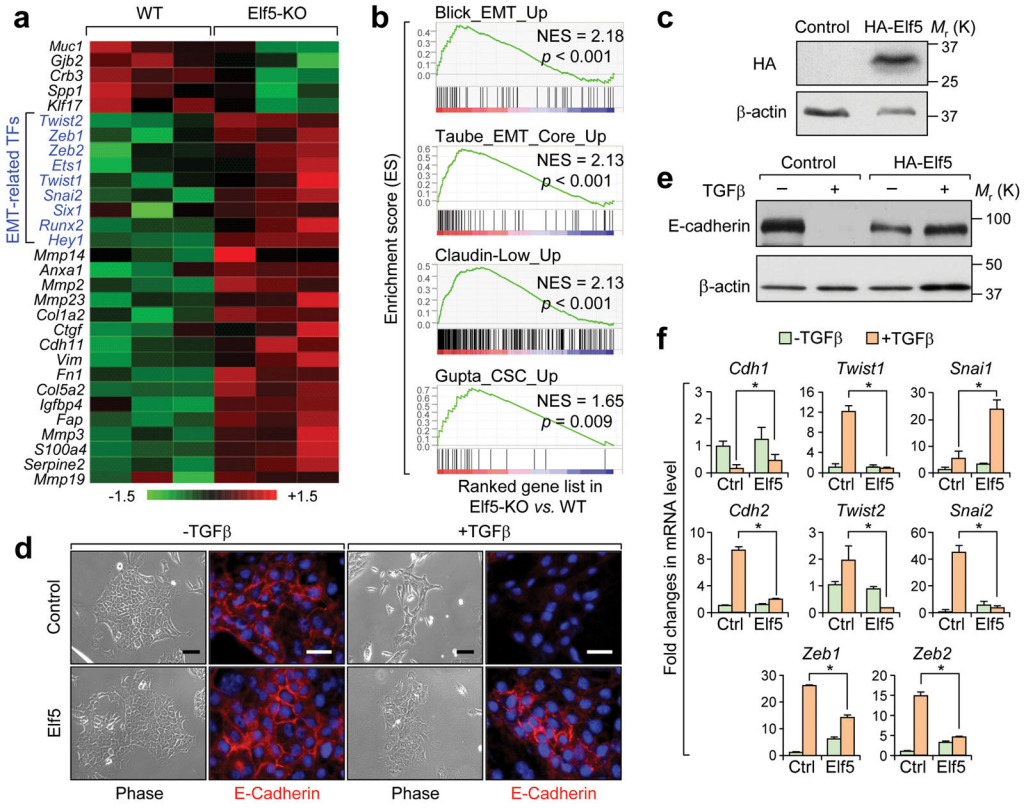

Figure 2. Loss of Elf5 leads to increased EMT gene expression programs

(a) Heat map representation of microarray data displaying the expression of several key EMT-related genes in wild type and Elf5-KO mammary glands on lactation day 1. ***(b)*** GSEA data showing the enrichment of four published EMT gene signatures[38-41] in Elf5-KO mammary glands as compared to wild type glands. NES: normalized enrichment score. ***(c, e)*** Western blot analyses of HA-Elf5 and E-cadherin protein levels in NMuMG cells transduced with vector (control) or HA-Elf5. Uncropped images of blots are shown in Supplementary Fig. S9. ***(d)*** Phase contrast and E-cadherin immunofluorescence images of NMuMG (control) or NMuMG-Elf5 cells undergoing TGFβ-induced EMT when cultured in low cell density. Experiments using cells cultured in high density are shown in Supplementary Fig. S1i. Size bar = 100 μm for brightfield and 40 μm for E-cadherin. ***(f)*** qRT-PCR analysis of expression of EMT-related genes in NMuMG (control) or NMuMG-Elf5 cells, with or without TGFβ treatment. Real time PCR values were normalized to the housekeeping gene *Gapdh*. Experiments were performed three times, each with qRT-PCR in technical duplicate, and data presented as the mean ± SD. * $p < 0.05$ by Student's t-test.

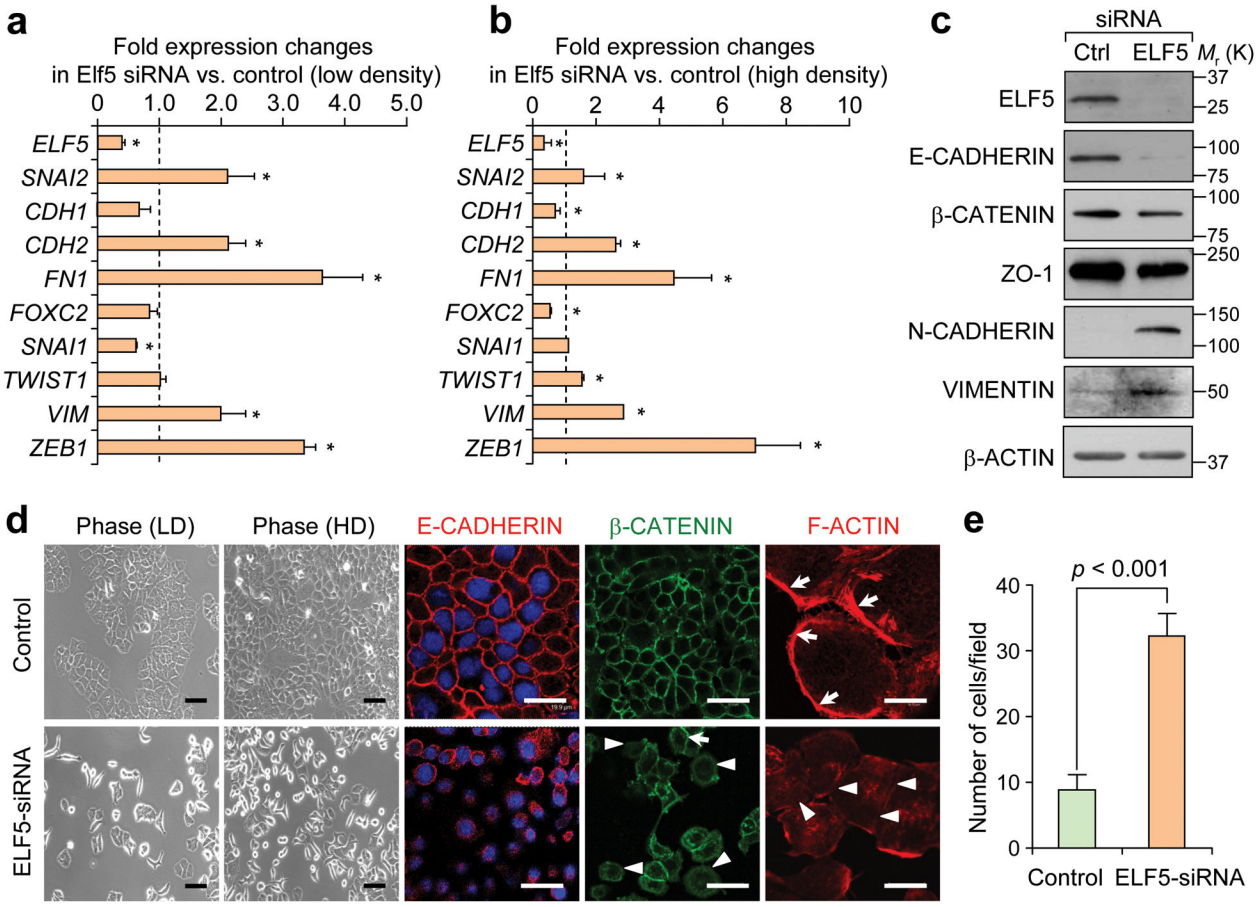

Figure 3. Silencing of ELF5 induces EMT in T47D cells and increases migratory potential

(a, b) Quantitative RT-PCR analysis of *ELF5* and EMT-related genes in T47D cells treated with control or ELF5 siRNA at low (***a***) or high (***b***) cellular density. Real time PCR values were normalized to the housekeeping gene *GAPDH*. Experiments were performed three times, each with qRT-PCR in technical duplicate, and data presented as the mean ± SD. * $p < 0.05$ by Student's t-test. ***(c)*** Western blot analysis of ELF5 and EMT markers in T47D cells treated with control or ELF5 siRNA. Uncropped images of blots are shown in Supplementary Fig. S9. ***(d)*** Phase contrast and immunofluoresence images of control or ELF5-knockdown T47D cells stained for E-CADHERIN, β-CATENIN, and F-ACTIN. Loss of F-actin circumferential belts (arrows) and relocalization of β-CATENIN from adherens junctions of the membrane (arrows) to cytoplasm are highlighted with arrowheads. Size bar = 100 μm for brightfield images and β-CATENIN, and 20 μm for E-CADHERIN and 18 μm for F-actin. See Supplementary Fig. S3a which shows the unchanged morphology of T47D cells after mock transfection. ***(e)*** Transwell migration assay of T47D cells with or without ELF5 knockdown. The data represented are shown as mean ± SD collected from 6 fields of 3 independent experiments. Student's t-tests were performed to assess statistical significance.

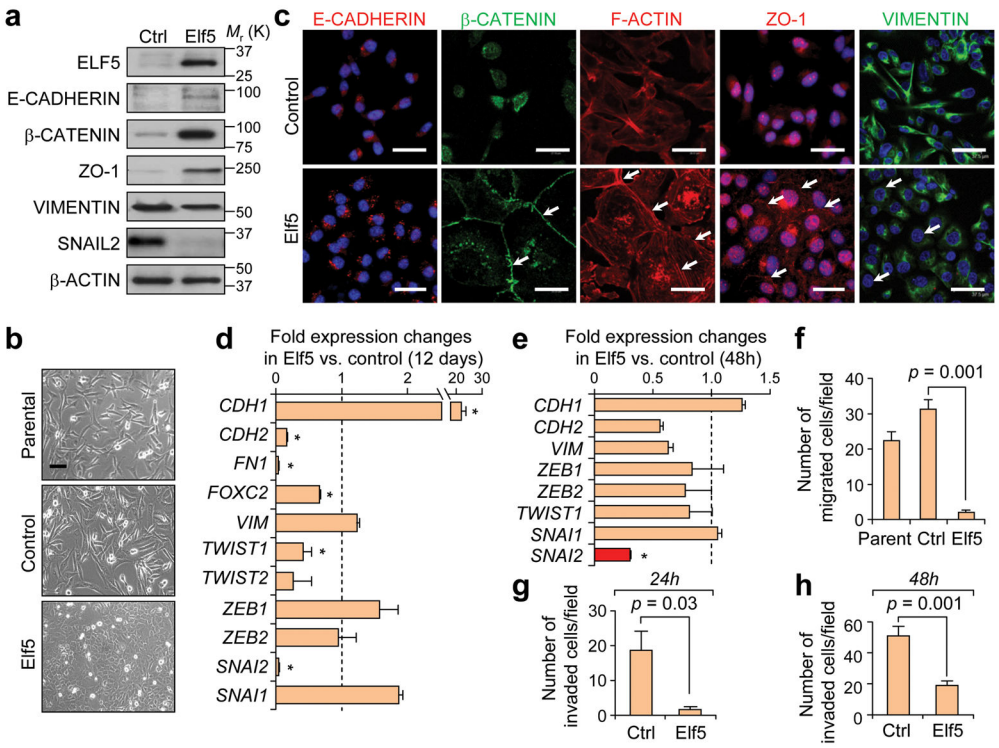

Figure 4. Overexpression of Elf5 reverses mesenchymal characteristics of MDA-231 cells

(a) Western blot analyses of HA-Elf5 and other EMT markers in MDA-231 cells transduced with vector (control) or HA-Elf5. Uncropped images of blots are shown in Supplementary Fig. S9. ***(b)*** Phase contrast images of parental, control or HA-Elf5-overexpressing MDA-231cells. Size bar = 100 μm. ***(c)*** Immunofluorescence analysis of control and HA-Elf5-overexpressing MDA-231 cells stained for the indicated proteins. Arrows mark the relocalization of nuclear β-CATENIN to the membrane and cytoplasm, restoration of circumferential F-actin belts, membrane localization of ZO-1 and adherens junctions, and reduced expression of VIMENTIN in Elf5-overexpressing cells. Size bar = 20 μm for β-CATENIN, and F-ACTIN, 60 μm for E-CADHERIN, and 40 μm for ZO-1 and VIMENTIN. ***(d, e)*** Quantitative RT-PCR analysis of the expression of EMT-related genes in control or HA-Elf5-overexpressing MDA-231 cells at 12 days ***(d)*** or 48h post-infection ***(e)***. Real time values were normalized to the housekeeping gene *GAPDH*. Experiments were performed three times, each with qRT-PCR in technical duplicate, and data presented as the mean ± SD. * $p < 0.05$ by Student's t-test. ***(f)*** Transwell migration assay of MDA-231 cells with or without Elf5 overexpression. The data are shown as mean ± SD collected from 10 fields of 3 independent experiments. Student's t-tests were performed to assess statistical significance. ***(g, h)*** Matrigel invasion assay of MDA-231 cells with or without Elf5 overexpression. Two time points were observed for invasion assays (24 h in ***g*** and 48 h in ***h***). The data were collected from 10 fields, performed in triplicate, and shown as mean ± SD. * $p < 0.05$ by Student's t-test.

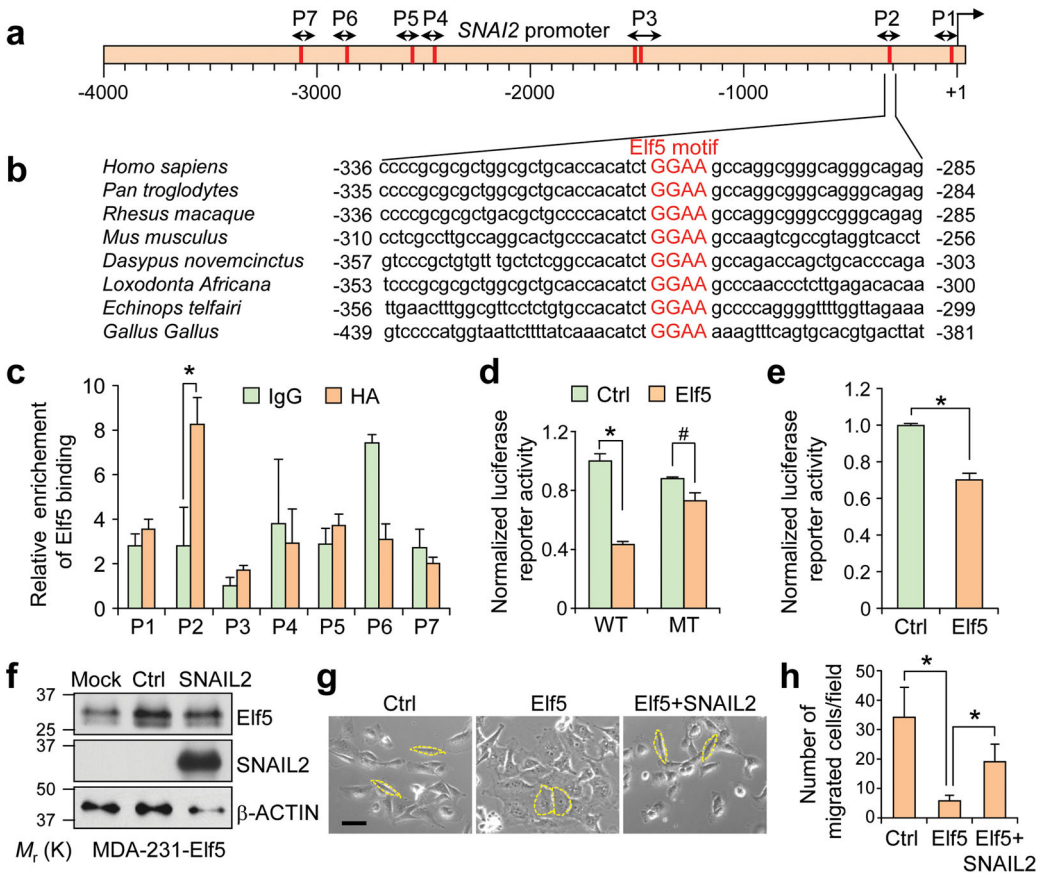

Figure 5. Elf5 binds to the *SNAI2* promoter and represses its expression

(a) Schematic depiction of the *SNAI2* promoter with several putative ELF5 binding sites (red boxes) indicated. Primer sets for ChIP analyses are indicated by the arrows in the schematic diagram. ***(b)*** Evolutionary conservation of the ELF5 binding motif in the P2 promoter-proximal region of the *SNAI2* gene. ***(c)*** ChIP analysis of HA-Elf5 binding to the *SNAI2* promoter in MDA-231-Elf5 cells. Quantitative PCR was performed with primers specific to seven regions on the *SNAI2* promoter as indicated in ***a***. Primers against the -300 bp promoter region (P2) show significant enrichment after normalization to the *GAPDH* control. Experiments were performed three times, each with qRT-PCR in technical duplicate, and data presented as the mean ± SD. ***(d)*** Relative expression of WT or mutant (MT) *SNAI2* promoter-driven luciferase reporters in control or Elf5-overexpressing MDA-231 cells. The data represented are shown as mean ± SD collected from 3 independent experiments. ***(e)*** Relative expression of a wild type (WT) *SNAI2* promoter-driven luciferase reporter in MCF-7 cells transiently transfected with vector control or HA-Elf5 expression plasmids. The data represented are shown as mean ± SD collected from 3 independent experiments. ***(f)*** Western blot of Elf5 and SNAIL2 protein levels in MDA-231-Elf5 cells transduced with vector (control) or *SNAI2*. Uncropped images of blots are shown in Supplementary Fig. S9. ***(g)*** Phase contrast images showing morphological characteristics of control, Elf5, or HA-Elf5 and FLAG-SNAIL2 overexpressing MDA-231 cells. Outlined cells demonstrate spindle-like (left and right) or cobblestone-like (middle) morphologies. Size bar = 10 μm ***(h)*** Transwell migration assay with control, Elf5, or Elf5 and SNAIL2 overexpressing

MDA-231cells. Data are shown as mean ± SD collected from 10 fields of 3 independent experiments. Student's t-tests were performed to assess statistical significance in ***c***, ***d***, ***e***, and ***h***. * $p < 0.05$ by Student's t-test; # $p > 0.05$.

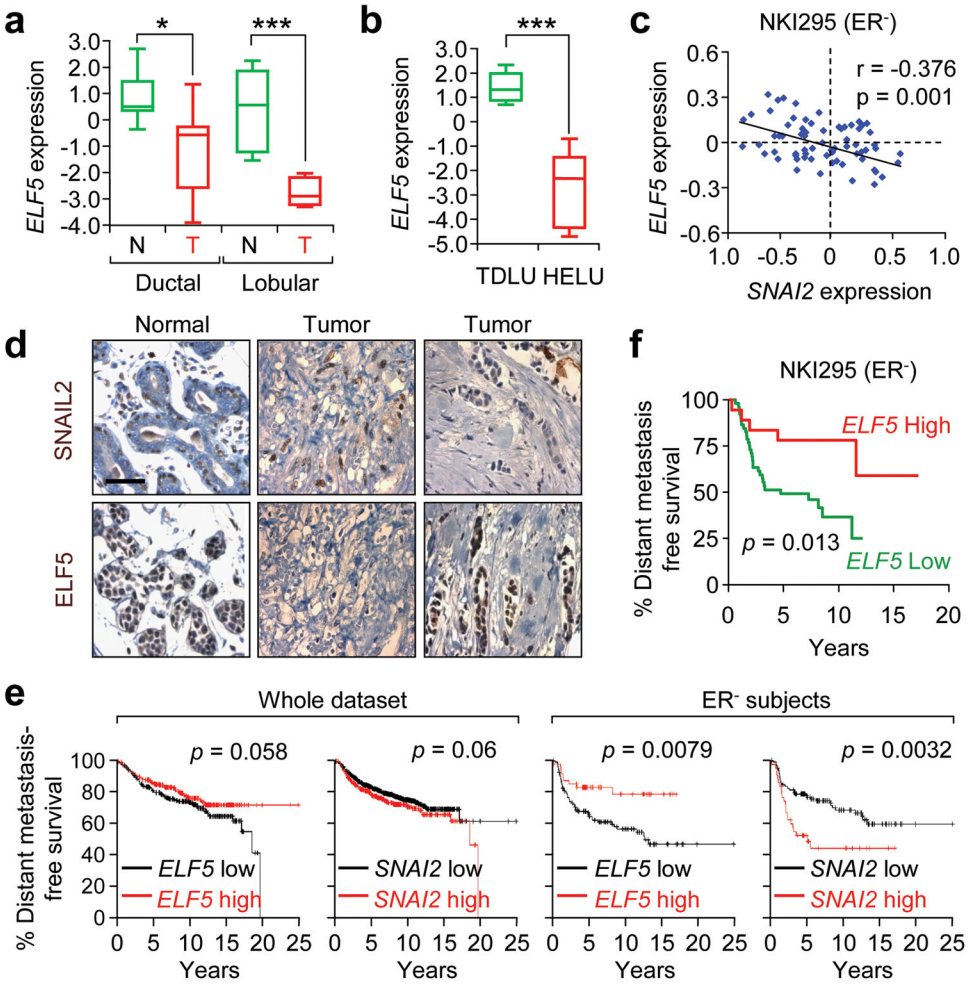

Figure 6. Expression pattern and prognostic values of ELF5 and SNAIL2 in breast tumors

(a) Box plots showing *ELF5* expression in laser capture microdissection samples of invasive ductal and lobular carcinomas as compared to normal ductal and lobular cells from matched mammary glands[46]. ***(b)*** Box plots showing *ELF5* expression in laser capture microdissection samples of hyperplastic enlarged lobular units (HELU) as compared to normal terminal duct lobular units (TDLU)[47]. ***(c)*** Scatter plot showing negative correlation between *SNAI2* and *ELF5* expression in ER- patients in the NKI295 clinical dataset. Pearsons' coefficient tests were performed to assess statistical significance. ***(d)*** IHC analysis showing ELF5 expression in luminal cells and SNAIL2 expression only in some basal cells in normal breast tissue (left panel). In human breast tumors, ELF5 and SNAIL2 show inverse correlation in expression (middle and right panels). Size bar = 20 μm. ***(e)*** Kaplan-Meier plots of distant metastasis-free survival of patients, stratified by expression of *Elf5* or *SNAI2*. Data obtained from the KM plotter database[49]. p value calculated by log rank test. ***(f)*** Kaplan-Meier plots of distant metastasis-free survival of ER- patients stratified by *Elf5* expression in the NKI295 clinical dataset. p value calculated by log rank test.

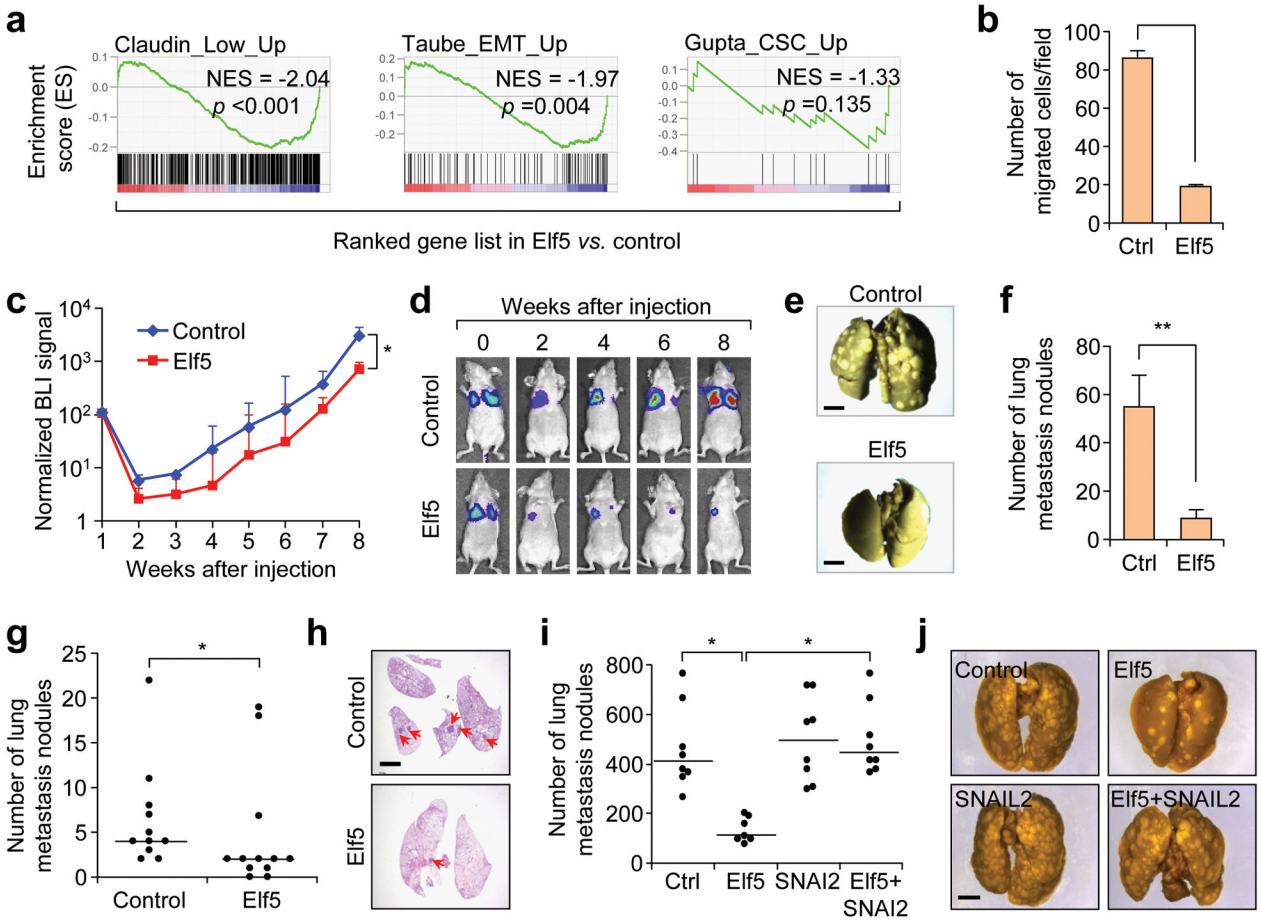

Figure 7. Elf5 inhibits lung metastasis in transplantable mouse models of metastasis

(a) GSEA showing negative enrichment of published EMT gene signatures[38-41] in Elf5-LM2 compared to control cells. ***(b)*** Transwell migration assay of control or HA-Elf5 overexpressing LM2 cells. Data are shown as mean ± SD from triplicate experiments. *p < 0.05 by Student's t-test. ***(c)*** Normalized BLI signals of lung metastases of mice (n = 8) injected intravenously with control or Elf5-overexpressing LM2 cells. Data represent average ± SEM. *p < 0.05 based on Mann-Whitney U test. ***(d)*** Representative BLI images of animals in each experimental group at the indicated time points. ***(e–f)*** Gross images ***(e)*** and quantification ***(f)*** of lung metastatic nodules from animals injected intravenously with control or Elf5-overexpressing LM2 cells. Size bar = 2 mm. **p < 0.01 by Student's t-test. ***(g)*** Box plot showing the number of lung metastasis nodules from spontaneous metastases generated by control or Elf5 overexpressing 4T1 cells after mammary fat pad injection (n=12). p = 0.0455 calculated by Mann-Whitney U test. ***(h)*** Representative H&E stained lung sections. Arrows highlight metastatic nodules. Size bar = 2 mm. ***(i)*** Box plot showing number of lung metastasis nodules from experimental metastasis of control, HA-Elf5, or HA-Elf5 and FLAG-SNAIL2 overexpressing 4T1 cells. *p < 0.05 by Student t- test. ***(j)*** Represented gross images of lung nodules. Size bar = 2 mm.

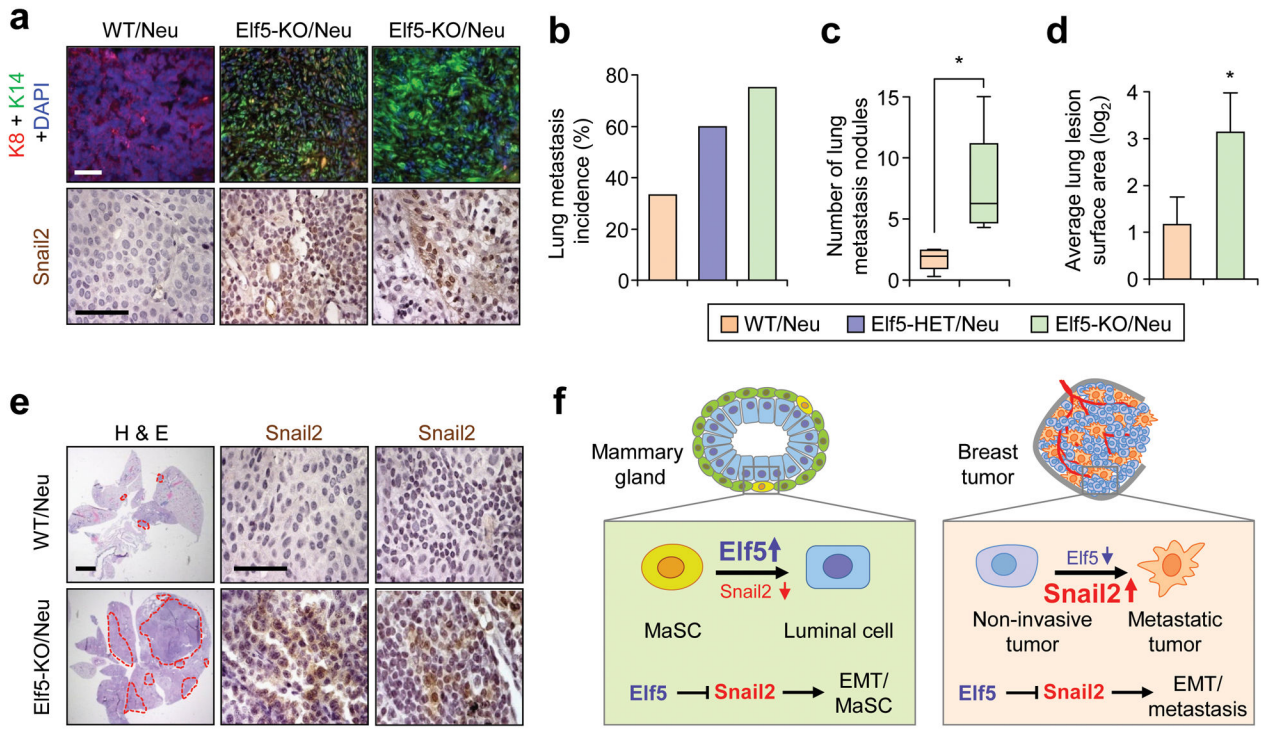

Figure 8. Elf5 inhibits lung metastasis in MMTV-Neu transgenic mouse model

(a) Primary mammary tumors stained with K14 and K8 or Snail2 from WT/MMTV-Neu+ or Elf5-KO/MMTV-Neu+ animals. Bar = 40 μm. ***(b–d)*** Lung metastasis incidence (***b***), number of lung metastasis lesions (***c***) and average lung lesion surface area (***d***) (arbitrary units based on pixel quantification from digital images, the data represented are shown as mean ± SD) from WT/MMTV-Neu+, Elf5-Het/MMTV-Neu+ and Elf5-cKO/MMTV-Neu+ animals (n = 11). p = 0.141 by Fisher Exact test in ***b***. p = 0.020 by Mann Whitney test in ***c***. p =0.025 by Student's t-test in ***d.*** ***(e)*** Snail2 staining in lung lesions from WT/MMTV-Neu+ or Elf5-KO/MMTV-Neu+ mice. Size bar = 2 mm and 40 μm for lung H & E and Snail2 IHC images respectively. ***(f)*** Schematic model for function of the Elf5-Snail2 axis in mammary cell fate regulation and breast cancer metastasis. During luminal differentiation of mammary epithelium, high expression of Elf5 in the differentiated luminal lineage suppresses Snail2 expression to inhibit mammary stem and progenitor cell properties (left). Low expression or loss of Elf5 allows Snail2 to induce EMT and increases Snail2-dependent stem and progenitor activities in the mammary gland (left), and promotes breast cancer invasion, metastasis, and potentially tumor initiating cell properties (right).